

Elastic properties and magnetic phase diagrams of dense Kondo compound $\text{Ce}_{0.75}\text{La}_{0.25}\text{B}_6$

Osamu SUZUKI, Shintaro NAKAMURA¹, Mitsuhiro AKATSU²,
Yuichi NEMOTO², Terutaka GOTO² and Satoru KUNII³

National Institute for Materials Science, Tsukuba 305-0047

¹Center for Low Temperature Science, Tohoku University, Sendai 980-8577

²Graduate School of Science and Technology, Niigata University, Niigata 950-2181

³Department of Physics, Tohoku University, Sendai 980-8578

(Received February 8, 2022)

We have investigated the elastic properties of the cubic dense Kondo compound $\text{Ce}_{0.75}\text{La}_{0.25}\text{B}_6$ by means of ultrasonic measurements. We have obtained magnetic fields vs. temperatures ($H-T$) phase diagrams under magnetic fields along the crystallographic [001], [110] and [111] axes. An ordered phase IV showing the elastic softening of c_{44} locates in low temperature region between 1.6 K and 1.1 K below 0.7 T in all field directions. The phase IV shows an isotropic nature with regard to the field directions, while the antiferromagnetic phase III shows an anisotropic character. A remarkable softening of c_{44} and a spontaneous trigonal distortion " $\epsilon_{yz} + \epsilon_{zx} + \epsilon_{xy}$ " recently reported by Akatsu et al. in the phase IV favor a ferro-quadrupole (FQ) moment of $O_{yz} + O_{zx} + O_{xy}$ induced by an octupole ordering.

KEYWORDS: $\text{Ce}_{0.75}\text{La}_{0.25}\text{B}_6$, elastic constant, ultrasonic measurement, quadrupolar ordering, octupolar ordering, magnetic phase diagram, dense Kondo effect

1. Introduction

CeB_6 and its substitutional compound $\text{Ce}_x\text{La}_{1-x}\text{B}_6$ are well known as the typical examples showing multipolar orderings and the dense Kondo effect. In CeB_6 the Hund's ground multiplet $^2F_{5/2}$ of Ce^{3+} splits into a quartet γ_8 ground state and a doublet γ_7 excited state located at 540 K in the cubic crystal-field (CEF).^{1,4} The CEF ground state of $\text{Ce}_x\text{La}_{1-x}\text{B}_6$ is also considered to be a quartet γ_8 from the results of the magnetic susceptibility measurements.⁴ Because of the large CEF splitting energy, the low-temperature properties of $\text{Ce}_x\text{La}_{1-x}\text{B}_6$ are dominated by the ground state quartet γ_8 with SU(4) symmetry. The direct product $\gamma_8 \otimes \gamma_8$ possesses fifteen quantum degrees of freedom consisting of three magnetic dipoles, five electric quadrupoles, and seven magnetic octupoles.⁵ Actually CeB_6 undergoes successive transitions from higher temperature paramagnetic phase I into an antiferro-quadrupolar (AFQ) phase II at $T_Q = 3.3$ K and further into an antiferromagnetic (AFM) phase III below $T_N = 2.3$ K in which the AFQ ordering coexists.^{6,7}

Present address: National Institute for Advanced Industrial Science and Technology, Tsukuba.

For a few decades, the AFQ phase II of CeB_6 has attracted much attention because of its order parameter and unusual magnetic field dependence of the AFQ transition temperature T_Q , whose behavior cannot be interpreted in terms of the conventional AFM ordering. With increasing magnetic fields, the transition point T_Q for the AFQ phase II shifts to higher temperatures. The result of neutron diffraction on CeB_6 indicates a field-induced AFM moments with a single wave vector $\mathbf{k} = \frac{1}{2}; \frac{1}{2}; \frac{1}{2}$ in the phase II, which was considered to be evidence of the AFQ ordering.⁷ However, the internal magnetic field in the phase II obtained by ^{11}B NMR measurements was interpreted as a triple- \mathbf{k} AFM structure.⁸ In order to solve this inconsistency between the neutron diffraction and NMR experiments, the influence of a field-induced antiferro-octupole (AFO) has been taken into consideration.⁹ The splitting and angular dependence of NMR signals have been explained by the hyperfine coupling between the nuclear spin of ^{11}B and the magnetic octupole moment of T_{xyz} of $\text{Ce} 4f$ -electron possessing the anti-parallel arrangement as same as the O_{xy} -AFQ ordering with a wave vector $\mathbf{k} = \frac{1}{2}; \frac{1}{2}; \frac{1}{2}$. The mean-field calculation including the AFO interaction by Shiina et al. reproduces well the experimental observation that the AFQ transition point T_Q increases considerably in magnetic fields. Their calculation indicates that the AFQ phase II is indeed stabilized by the AFO interaction in high magnetic fields.^{5,10,13}

The substitution of non-magnetic lanthanum ions for magnetic cerium ones in $\text{Ce}_x\text{La}_{1-x}\text{B}_6$ modifies drastically the magnetic phase diagram at low temperatures (low T) in low magnetic field (low H) region. The quadrupolar interaction for the AFQ phase II reduces much faster than the magnetic dipolar interaction for the AFM phase III as reducing the cerium concentration x . A new ordered phase IV manifests itself in the compound $\text{Ce}_{0.75}\text{La}_{0.25}\text{B}_6$ in addition to the AFQ phase II and AFM phase III.^{14,16} The specific heat of $\text{Ce}_{0.75}\text{La}_{0.25}\text{B}_6$ in the zero magnetic field shows a sharp peak at $T_{c1} = 1.6$ K and a small one at $T_{c2} = 1.1$ K. The magnetic susceptibility in the phase IV of $\text{Ce}_{0.75}\text{La}_{0.25}\text{B}_6$ is quite isotropic with respect to the magnetic field directions along the three principal [001], [110] and [111] axes.¹⁵ It is difficult to explain these unusual characteristics in terms of the conventional AFM ordering.

Recently, several microscopic measurements have been performed on $\text{Ce}_x\text{La}_{1-x}\text{B}_6$ in the phase IV. No indication of AFM ordering in the phase IV was found by the neutron scattering of powder samples.¹⁷ The NMR and muon spin relaxation measurements on $\text{Ce}_x\text{La}_{1-x}\text{B}_6$ ($x = 0.7$) indicate the breaking of the time reversal symmetry in the phase IV.^{18,19} Quite recently, Aikawa et al. measured the thermal expansion of $\text{Ce}_x\text{La}_{1-x}\text{B}_6$ ($x = 0.75, 0.70$) at low temperatures.²⁰ They successfully found that in the phase IV the lattice expands along the [001] axis, while shrinks along the [111] axis. This result provides an evidence for a trigonal lattice distortion due to the spontaneous strain $h''_{yz} = h''_{zx} = h''_{xy} = 5 \times 10^{-6}$ in the phase IV below T_{c1} . This tiny but definite distortion promises the fact that the ferro-quadrupole moment $hO_{yz} = hO_{zx} = hO_{xy}$ is relevant in the phase IV. The phase IV of $\text{Ce}_{0.70}\text{La}_{0.30}\text{B}_6$

below $T_{c1} = 1.4$ K is stable down to absolute zero without showing the AFM phase III.^{15,21}

In the more diluted system $Ce_xLa_{1-x}B_6$ at $x = 0.60$, the inter-site interactions for the AFQ phase II and the AFM phase III considerably reduces, although the Kondo temperature (T_K) of about 1 K is almost independent of the cerium concentration x .²² In the compounds $x = 0.60$ and 0.50 , the dense Kondo effect, therefore, may play a dominant role to realize the non-magnetic state in low T , low H region.²³

The anisotropy of the elastic properties of $Ce_{0.75}La_{0.25}B_6$ in magnetic fields has not been investigated in detail so far. In order to elucidate the characteristics of the phase IV, we have investigated the elastic properties and magnetic phase diagram of $Ce_{0.75}La_{0.25}B_6$ in magnetic fields along the three principal [001], [111] and [110] axes by ultrasound measurements. We also discuss the order parameter in the phase IV from the elastic properties and magnetic phase diagrams of $Ce_{0.75}La_{0.25}B_6$.

2. Experimental details

A single crystal of $Ce_{0.75}La_{0.25}B_6$ was grown by the coating zone method. We cut the specimen of $Ce_{0.75}La_{0.25}B_6$ into a $4.8 \times 5.3 \times 6.0$ mm³ rectangular shape. The specimen used in the present experiment is the same one used in ref. 10. We measured elastic constants by means of an ultrasonic apparatus based on the phase comparison technique.²⁴ The parallel faces of the specimen perpendicular to the high symmetry [001], [111] and [110] axes were polished by fine powder of carborundum. A pair of ultrasonic transducers made of $LiNbO_3$ plates were bonded on the parallel end faces of the specimen by RTV silicone rubber (Shin-Etsu Chemical Co., Ltd.). The propagation vector k and the polarization one u of sound wave are chosen as $k // u // [001]$ for c_{11} , $k // [110]$ and $u // [110]$ for $(c_{11} - c_{12})/2$, $k // [001]$ and $u // [100]$ for c_{44} , respectively. We used a longitudinal ultrasonic wave with 8 MHz and a transverse one with 10 MHz. We employed a sample-immersed ³He-evaporation refrigerator equipped with a 12 T-superconducting magnet (Oxford Instruments Co., Ltd.) for the low-temperature measurements in magnetic fields.

3. Experimental Results

The temperature dependences of c_{44} in $Ce_{0.75}La_{0.25}B_6$ under various magnetic fields along [001], [110], and [111] axes are shown in Figs. 1-3, respectively. In Fig. 1, we cited the previous results in fields along the [001] axis for comparison.¹⁴ In the paramagnetic phase I under zero magnetic field, c_{44} softens slightly due to the quadrupole-strain interaction with the antiferro-type quadrupole inter-site interaction $g_5^0 = 2$ K.¹⁴ c_{44} turns to huge softening in phase IV below T_{c1} (~ 1.6 K) and increases rapidly below T_{c2} (~ 1.1 K). Here T_{c1} and T_{c2} denotes the transition temperature from the paramagnetic phase I to the phase IV and that from the phase IV to the AFM phase III, respectively. We identify the transition point T_{c1} with the onset of the softening of c_{44} and T_{c2} with the increase of c_{44} . With increasing magnetic fields,

the softening of c_{44} reduces rapidly and T_{c2} shifts to higher temperatures. At $H = 1.0$ T, the softening in c_{44} almost vanishes. This means that the phase IV disappears and another phase II emerges. A small dip is observed at the AFM transition point T_N in three magnetic field directions as shown in Figs. 1–3.

The transverse $(c_{11} - c_{12})/2$ mode also exhibits anomalies around the I–IV phase transition point. Fig. 4 shows the temperature dependence of $(c_{11} - c_{12})/2$ of $\text{Ce}_{0.75}\text{La}_{0.25}\text{B}_6$ under various magnetic fields along the [110] axis. In zero magnetic field, $(c_{11} - c_{12})/2$ shows a slight softening in paramagnetic phase I toward a sharp minimum at $T_{c1} = 1.6$ K. $(c_{11} - c_{12})/2$ also shows a bending at T_{c2} in zero magnetic field, which corresponds to the transition from the phase IV to the AFM phase III". No softening of $(c_{11} - c_{12})/2$ in the phase IV is in contrast to the huge softening of c_{44} . With increasing magnetic fields up to 0.7 T, the temperature range of the phase IV becomes narrower. Under the fields of 1.0 T and 1.5 T, the phase IV disappears. $(c_{11} - c_{12})/2$ shows a small bending at the AFQ transition points T_Q . A sharp reduction of $(c_{11} - c_{12})/2$ at the transition point to the AFM phase III' and an increase of $(c_{11} - c_{12})/2$ at the transition point to the phase III have clearly been observed.

The temperature dependence of the longitudinal c_{11} of $\text{Ce}_{0.75}\text{La}_{0.25}\text{B}_6$ under magnetic fields along the [111] axis is shown in Fig. 5. The transition temperature T_{c2} indicated by downward arrows shifts to higher temperatures with increasing magnetic fields. In contrast to T_{c2} , T_{c1} indicated by upward arrows is almost independent of magnetic field. Under the field of 2.0 T, the phase IV disappears and the AFQ phase II appears. Similar to the case of $(c_{11} - c_{12})/2$, c_{11} shows a small decrease in the phase IV.

Fig. 6 shows the field dependence of $(c_{11} - c_{12})/2$ of $\text{Ce}_{0.75}\text{La}_{0.25}\text{B}_6$ along the [110] axis at various fixed temperatures. At temperatures higher than 1.6 K, the inflection in $(c_{11} - c_{12})/2$ indicated by arrows shows the transition points T_Q from the paramagnetic phase I to the AFQ phase II. In the temperature range $1.1 \text{ K} < T < 1.6 \text{ K}$, $\text{Ce}_{0.75}\text{La}_{0.25}\text{B}_6$ undergoes a successive transition from the phase IV to the AFM phase III, AFM sub-phase III' and AFQ phase II with increasing magnetic fields. The observed hysteresis in the field dependence at 1.4 K indicates the transition between the phase IV and the phase III to be of first-order as reported by magnetic susceptibility measurements by Tayama et al.¹⁵ At 1.21 K, the phase III" was found in a very narrow field range. The results of c_{44} in Fig. 1 and c_{11} in Fig. 5 have already shown that the phase III" appears in zero magnetic field below 1.1 K. At the lowest temperature 0.54 K, $\text{Ce}_{0.75}\text{La}_{0.25}\text{B}_6$ exhibits the successive transitions from the AFM sub-phase III" to the AFM phase III indicated by a hysteretic profile below 1 T. A step-like increase at around 2 T corresponds to the AFM sub-phase III'. At around 2.5 T, $(c_{11} - c_{12})/2$ shows a discontinuous increase, which indicates the transition from the AFM phase III' to AFQ phase II.

In Fig. 7, we show the temperature dependence of c_{44} in $\text{Ce}_{0.75}\text{La}_{0.25}\text{B}_6$ in fields above 6 T

applied parallel to the $[110]$ axis. Sharp bending points in c_{44} are the indication of T_Q for the AFQ transition from the paramagnetic phase I. With decreasing temperature, c_{44} shows the Curie-Weiss-type softening with a negative (antiferro) inter-site quadrupole interaction.¹⁴ c_{44} shows upturns at T_Q indicated by arrows. The increase of c_{44} below T_Q in Fig. 7 is a common feature associated with the AFQ ordering. The AFQ transition temperature T_Q shifts to higher temperatures with increasing magnetic fields up to 12 T.

Next we show the temperature dependence of c_{11} of $\text{Ce}_x\text{La}_{1-x}\text{B}_6$ in fields above 5 T along the $[111]$ axis in Fig. 8. The sharp bending points of c_{11} indicated by arrows in Fig. 8 correspond to the transition points T_Q from the phase I to the AFQ phase II. The transition temperature T_Q shifts to higher temperatures with increasing field.

Taking together the above-mentioned results, we obtained the magnetic phase diagrams of $\text{Ce}_{0.75}\text{La}_{0.25}\text{B}_6$ under the magnetic fields parallel to the three principal axes as shown in Fig. 9. In these phase diagrams, the AFQ phase II spreads to high fields, the AFM phase III, III' and III'' occupies the low- T , low- H region, while the phase IV appears only in narrow temperature regions under low magnetic fields. The boundary $T_Q(H)$ between the phase I and the phase II for $H \parallel [001]$ stays slightly lower temperature regions than those under $H \parallel [111]$ and $H \parallel [110]$. In fields of $H \parallel [111]$ and $H \parallel [110]$ $T_Q(H)$ are quite close to each other. This anisotropy of the AFQ phase II is consistent with the theoretical calculation on CeB_6 in low- H region.^{5,10} The critical field between the AFM phase III' and the AFQ phase II at the lowest temperature in the present experiments is in order of $H_{[001]}^{\text{III}' \rightarrow \text{II}} > H_{[111]}^{\text{III}' \rightarrow \text{II}} > H_{[110]}^{\text{III}' \rightarrow \text{II}}$. Regardless of the field direction, the AFM phase below T_{c2} consists of the three sub phases III'', III and III' from the lower field side.

4. Discussion

In the present study, we found the enormous softenings of c_{44} in the phase IV of $\text{Ce}_{0.75}\text{La}_{0.25}\text{B}_6$ under magnetic fields along the three crystallographic $[001]$, $[111]$ and $[110]$ axes as shown in Figs. 1–3. On the other hands, other elastic modes $(c_{11} - c_{12})/2$ in Fig. 4 and c_{11} in Fig. 5 show a hardening or temperature independent behavior in the phase IV. The behavior of c_{44} around T_{c1} is distinguished from those around T_Q to the AFQ phase II (a small dip) or around T_{c2} to the AFM + AFQ phase III (a rapid increase). At the transition point from the paramagnetic phase I to the AFQ phase II, the elastic constants c_{11} and $(c_{11} - c_{12})/2$ show a sharp bending (Figs. 5, 7 and 8). However, c_{44} of $\text{Ce}_{0.75}\text{La}_{0.25}\text{B}_6$ in Figs. 1–3 shows the rapid decrease below T_{c1} with lowering temperatures in the absence of magnetic fields. c_{44} is described by the quadrupolar susceptibility associated with the quadrupole moments O_{yz} , O_{zx} and O_{xy} . The remarkable softening of c_{44} in the phase IV of $\text{Ce}_{0.75}\text{La}_{0.25}\text{B}_6$ is strictly distinguished from the bending of c_{44} at the transition point to the AFQ phase II in CeB_6 .

Recent thermal expansion measurement by Akatsu et al. have shown that the trigonal distortion $h''_{yz} = h''_{zx} = h''_{xy} = 5 \times 10^{-6}$ manifests itself in the phase IV of $\text{Ce}_x\text{La}_{1-x}\text{B}_6$

with $x = 0.75$ and 0.70 .²⁰ This result means that the ferro-quadrupole moment $\langle O_{yz} \rangle = \langle O_{zx} \rangle = \langle O_{xy} \rangle$ with T_h symmetry is relevant in the phase IV. The FQ ordering, namely the cooperative Jahn-Teller transition, is one of the plausible models to bring about the trigonal lattice distortion in general. In the case of the FQ ordering, however, a considerable elastic softening above T_Q is expected as a precursor of the elastic instability. As shown in Figs. 1-3, c_{44} of $\text{Ce}_{0.75}\text{La}_{0.25}\text{B}_6$ shows the softening of only 1 % above the transition point T_{c1} to the phase IV. Furthermore, the magnetic susceptibility is expected to be silent at the FQ transition point. The conventional FQ transition is unfavorable for the cusp of the magnetization upon the transition to the phase IV in the experimental results by Tayama et al.¹⁵

Very recently Kubo and Kuramoto proposed an octupole-ordering model to explain the unusual elastic and magnetic properties of the phase IV in $\text{Ce}_x\text{La}_{1-x}\text{B}_6$.^{25,26} This model shows that the antiferro-octupole-ordering of $T_x + T_y + T_z$ with T_h symmetry in their notation simultaneously induces the FQ moment $O_{yz} + O_{zx} + O_{xy}$, which naturally brings about a trigonal lattice distortion through the quadrupole-strain interaction. Their calculation results give a reasonable magnitude of the spontaneous strain being comparable to the result obtained by the thermal expansion measurements reported by Aikawa et al.²⁰ However, the behavior of c_{44} cannot be explained quantitatively by the octupolar model. The magnitude of a jump in c_{44} at $T_{c1} = 1.6$ K predicted by their model (0.92×10^{11} erg/cm³) is smaller than the observed softening (2.5×10^{11} erg/cm³) in the phase IV. The reason of this discrepancy may come from the neglect of the fluctuation effect in their model as pointed out by Kubo et al. Ideally, the second derivative of the free energy such as elastic constants shows a discontinuity when the phase transition is of second-order. However discontinuities are not observed in the elastic constants c_{44} of $\text{Ce}_{0.75}\text{La}_{0.25}\text{B}_6$ in the vicinity of the transition to the phase IV. We suppose that the absence of the discontinuity in the elastic constants is due to the quadrupolar fluctuation with T_h symmetry. The existence of the quadrupolar fluctuation with T_h symmetry is evident because the strong ultrasonic attenuation is observed in the echo signals of c_{44} . In addition, the inter-site octupolar interaction prevents the divergence of the quadrupolar susceptibility χ_4 , in other words, the elastic softening in c_{44} stops at finite values not at zero, which is consistent with the experimental results of c_{44} . The octupolar model proposed by Kubo et al. can explain the elastic properties in the phase IV of $\text{Ce}_{0.75}\text{La}_{0.25}\text{B}_6$ as the mentioned-above qualitatively at least. This model is the most plausible model among the proposed ones of the ordering mechanism in the phase IV up to now, because the elastic constant, thermal expansion and the magnetic susceptibility can be explained naturally. Recent magnetic susceptibility measurements in uni-axial pressure by Morie et al. also support the octupolar ordering model.²⁷ Furthermore, the breaking of the time reversal symmetry in the octupole ordering model may be consistent with the muon spin resonance and NMR experiment on the phase IV.^{18,19} The octupole ordering of $T_x + T_y + T_z$ lifts the t_2 quartet into a

singlet ground state, a first excited doublet state and a second excited singlet state. Hence the octupole ordered phase IV can be stable down to absolute zero. Actually in $\text{Ce}_{0.70}\text{La}_{0.30}\text{B}_6$ no phase transition except one at T_{c1} to the phase IV is observed down to 50 mK.²¹

As shown in Fig. 8, the phase IV in the H - T plane spreads as quite isotropic manner with respect to the magnetic field directions. The phase IV is easily destroyed by the weak magnetic field of 0.7 T. The AFM ordering temperature T_{c2} shifts to higher temperatures with increasing fields. The anisotropic field dependence of the AFM phase II is in contrast to the isotropic field dependence of the phase IV. The Kondo effect plays a role to screen the magnetic dipole moment in the AFM phases. Actually the tiny AFM component with the magnitude of about $0.25 \mu_B$ is observed in the phase III of $\text{Ce}_{0.75}\text{La}_{0.25}\text{B}_6$ by the neutron scattering.⁷ This is much smaller than the full moment of g state ($1.57 \mu_B$). Furthermore, the recent measurements by Nakamura et al. showed the T^2 -behavior in the temperature dependence of electrical resistivity in the phase IV of $\text{Ce}_{0.65}\text{La}_{0.35}\text{B}_6$.²⁸ This result suggests that the Fermi liquid state is realized by the dense Kondo effect in the phase IV of $\text{Ce}_x\text{La}_{1-x}\text{B}_6$.

5. Summary

We investigated the elastic properties of $\text{Ce}_{0.75}\text{La}_{0.25}\text{B}_6$ under magnetic fields by means of ultrasonic measurements. We obtained the magnetic phase diagrams of $\text{Ce}_{0.75}\text{La}_{0.25}\text{B}_6$ under fields along the three principal axes. The phase IV of $\text{Ce}_{0.75}\text{La}_{0.25}\text{B}_6$ is located only in the narrow temperature region. The phase IV spreads isotropically in H - T plane being independent of the field directions. The huge softening in c_{44} and the trigonal distortion of $\epsilon_{yz} + \epsilon_{zx} + \epsilon_{xy}$ in the phase IV showed that the FQ moment of $O_{yz} + O_{zx} + O_{xy}$ is relevant in the phase IV. The antiferro octupole ordering model of $T_x + T_y + T_z$ proposed by Kubo and Kuramoto is the most plausible way to describe the elastic properties as well as the magnetic ones in the phase IV.

References

References

- 1) E.Zimngiebl, B.Hillebrands, S.Blumenroder, G.Guntherodt, M.Loewenhaupt, J.M.Carpenter, K.Winzer and Z.Fisk :Phys.Rev.B 30 (1984) 4052 .
- 2) B.Luthi, S.Blumenroder, B.Hillebrands, G.Guntherodt, K.Winzer :Z.Phys.58 (1984) 31.
- 3) M.Loewenhaupt, J.M.Carpenter and C.-K.Loong:J.Magn.Magn.Mater. 52 (1985) 245.
- 4) N.Sato, S.Kunii, I.Oguro, T.Komatsubara and T.Kasuya:J.Phys.Soc.Jpn. 53 (1984) 3967.
- 5) R.Shina, H.Shiba and P.Thalmier: J.Phys.Soc.Jpn. 66 (1997) 1741 .
- 6) T.Fujita, M.Suzuki, T.Komatsubara, S.Kunii, T.Kasuya and T.Ohtsuka: Solid State Commun. 35 (1980) 569.
- 7) J.M.E antin, J.Rossat-M ignot, P.Burlet, H.Bartholin, S.Kunii and T.Kasuya:J.Magn.Magn.Mater. 47& 48 (1985) 145.
- 8) M.Takigawa, H.Yasuoka, T.Tanaka and Y.Ishizawa:J.Phys.Soc.Jpn. 52 (1983) 728.
- 9) O.Sakai, R.Shina, H.Shiba and P.Thalmier: J.Phys.Soc.Jpn. 66 (1997) 3005 .
- 10) R.Shina, O.Sakai, H.Shiba and P.Thalmier :J.Phys.Soc.Jpn. 67 (1998) 941.
- 11) M.Hiroi, S.Kobayashi, M.Sera, N.Kobayashi and S.Kunii:Phys.Rev.Lett. 81 (1998) 2510.
- 12) D.Hall and Z.Fisk and R.G.Goodrich :Phys.Rev.B 62 (2000) 84.
- 13) M.Akatsu, T.Goto, O.Suzuki, Y.Nemoto, S.Nakamura, S.Kunii and G.Kido :Phys.Rev.Lett. 93 (2004) 156409.
- 14) O.Suzuki, T.Goto, S.Nakamura, T.Matsumura and S.Kunii:J.Phys.Soc.Jpn. 67 (1998) 4243.
- 15) T.Tayama, T.Sakakibara, K.Tenya, H.Amitsuka and S.Kunii:J.Phys.Soc.Jpn. 66 (1997) 2268 .
- 16) M.Hiroi, M.Sera, N.Kobayashi and S.Kunii:Phys.Rev.B 55 (1997) 8339 .
- 17) K.Iwasa, K.Kuwahara, M.Kohgi, P.Fischer, A.Donni, L.Keller, T.C.Hansen, S.Kunii, N.Metoki, Y.Koike and K.Ohoyama :Physica B 329-333 (2003) 582.
- 18) H.Takagiwa, K.Ohishi, J.Akimitsu, W.Higemoto, R.Kadono, M.Sera and S.Kunii :J.Phys.Soc.Jpn. 71 (2002) 31.
- 19) K.Magishi, M.Kawakami, T.Saito, K.Koyama, K.Mizuno and S.Kunii :Z.Naturforsch A 57 (2002) 441.
- 20) M.Akatsu, T.Goto, Y.Nemoto, O.Suzuki, S.Nakamura and S.Kunii :J.Phys.Soc.Jpn. 72 (2003) 205.
- 21) Y.Nemoto, M.Akatsu, T.Goto, O.Suzuki, S.Nakamura and S.Kunii:Physica B 312-313 (2002) 191.
- 22) N.Sato, A.Sumiyama, S.Kunii, H.Nagano and T.Kasuya :J.Phys.Soc.Jpn. 54 1985 1923.
- 23) S.Nakamura, T.Goto, O.Suzuki, S.Kunii, and S.Sakatsume Phys.Rev.B 61, 15203 (2000).
- 24) B.Luthi : in Dynamical Properties of Solids (North-Holland Publishing Company, Amsterdam , 1980), ed. by G.K.Horton and A.A.Maradudin, Chap. 4.
- 25) K.Kubo and Y.Kuramoto :J.Phys.Soc.Jpn. 72 (2003) 1859.
- 26) K.Kubo and K.Kuramoto :J.Phys.Soc.Jpn. 73 (2004) 216.
- 27) T.Morie, T.Sakakibara, T.Tayama and S.Kunii :J.Phys.Soc.Jpn. 73 (2004) 2381.
- 28) S.Nakamura, M.Endo, H.Aoki, N.Kimura, T.Nojima and S.Kunii :Phys.Rev.B 68 (2003) 100402.

Figure captions

Fig.1. The elastic constants c_{44} of $\text{Ce}_{0.75}\text{La}_{0.25}\text{B}_6$ as functions of temperature under various magnetic fields along the [001] axis. The data are cited from ref11. Wave vector k and polarization one u of ultrasound are directed along the [001] axis and along the [100], respectively. Arrows are indications of phase transition points.

Fig.2. The elastic constants c_{44} of $\text{Ce}_{0.75}\text{La}_{0.25}\text{B}_6$ as functions of temperature under various magnetic fields along the [110] axis. Wave vector k and polarization one u of ultrasound are directed along the [110] axis and along the [001], respectively. Arrows are indications of phase transition points.

Fig. 3. The elastic constants c_{44} of $\text{Ce}_{0.75}\text{La}_{0.25}\text{B}_6$ as functions of temperature under various magnetic fields along the [111] axis. Wave vector k and polarization vector u of the ultrasound is directed along the [100] and [001] axes, respectively. Arrows are indication of the phase transition points.

Fig. 4. The elastic constant $(c_{11} - c_{12})/2$ of $\text{Ce}_{0.75}\text{La}_{0.25}\text{B}_6$ as functions of temperatures under various magnetic fields along the [110] axis. Wave vector k and polarization one u of ultrasound are directed along the [110] axis and [110] one, respectively. The origin of each data is shifted for clarity. Arrows are indication of the phase transition points.

Fig. 5. The elastic constant c_{11} of $\text{Ce}_{0.75}\text{La}_{0.25}\text{B}_6$ as functions of temperatures under various magnetic fields along the [111] axis. Both the wave vector k and polarization one u of the ultrasound are directed along the [100] axis. Upward and downward arrows indicate T_{c1} and T_{c2} , respectively. The origin of each data is shifted for clarity.

Fig. 6. The elastic constant $(c_{11} - c_{12})/2$ of $\text{Ce}_{0.75}\text{La}_{0.25}\text{B}_6$ as functions of magnetic field along the [110] axis at various temperatures. Wave vector k and polarization one u of ultrasound are directed along the [110] and [110] axes, respectively. The origin of each data is shifted for clarity. Arrows indicate phase transition points.

Fig. 7. The elastic constants c_{44} of $\text{Ce}_{0.75}\text{La}_{0.25}\text{B}_6$ as functions of temperatures under various magnetic fields along the [110] axis. Wave vector k and polarization one u of ultrasound is directed along the [110] and along the [001] axes, respectively. Arrows indicate the transition points from the paramagnetic phase I to the AFQ phase II.

Fig. 8. The elastic constant c_{11} of $\text{Ce}_{0.75}\text{La}_{0.25}\text{B}_6$ as functions of magnetic field along the [111] axis under various magnetic fields. Both the wave vector k and polarization one u of the ultrasound are directed along the [100] axis. The origin of each data is shifted for clarity. Arrows are indication of phase transition points.

Fig. 9. Magnetic phase diagrams of $\text{Ce}_{0.75}\text{La}_{0.25}\text{B}_6$ in H - T planes. Magnetic fields are directed along the (a) [001], (b) [111], (c) [110] axes, respectively. The phase I, II and III are the paramagnetic phase, antiferro-quadrupolar phase and antiferro-magnetic phase in which antiferro-quadrupolar order coexists, respectively. The phase III' and III'' are the sub-phase

of the antiferromagnetic phase III.

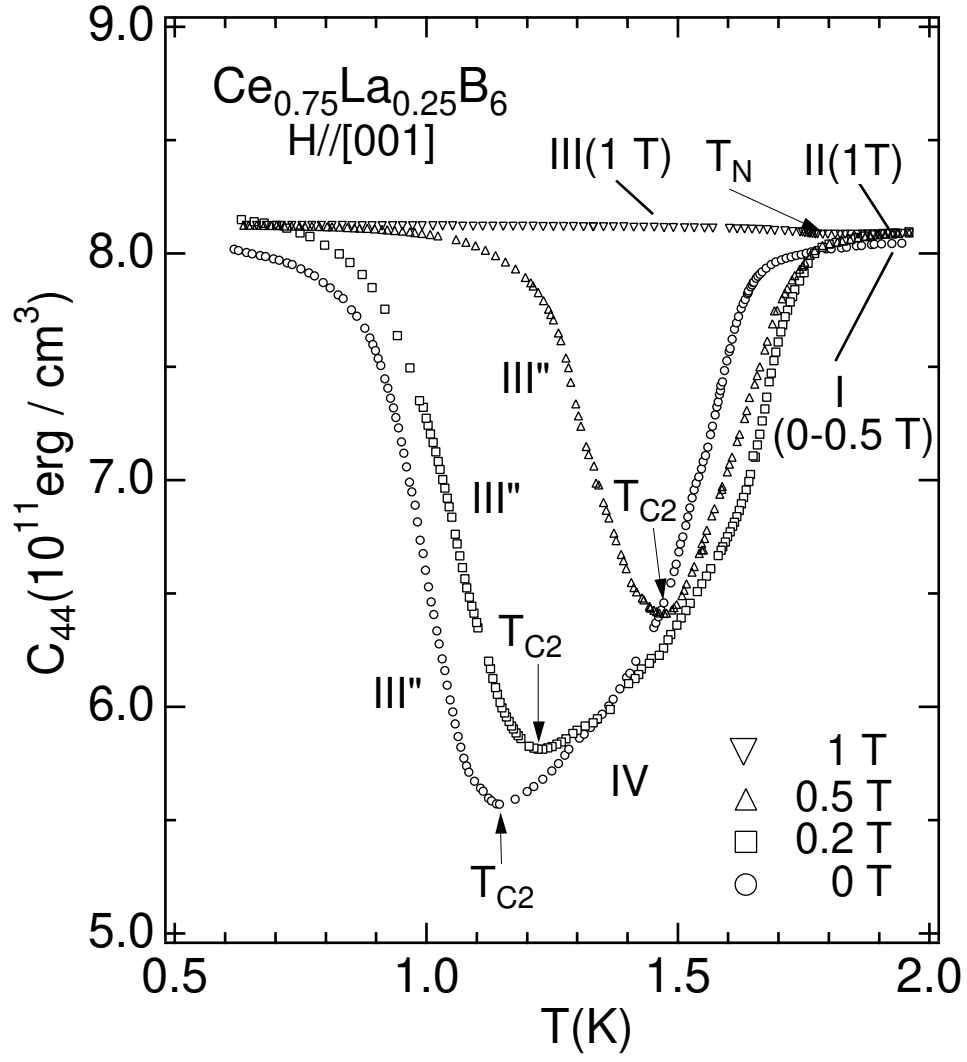


Fig. 1.

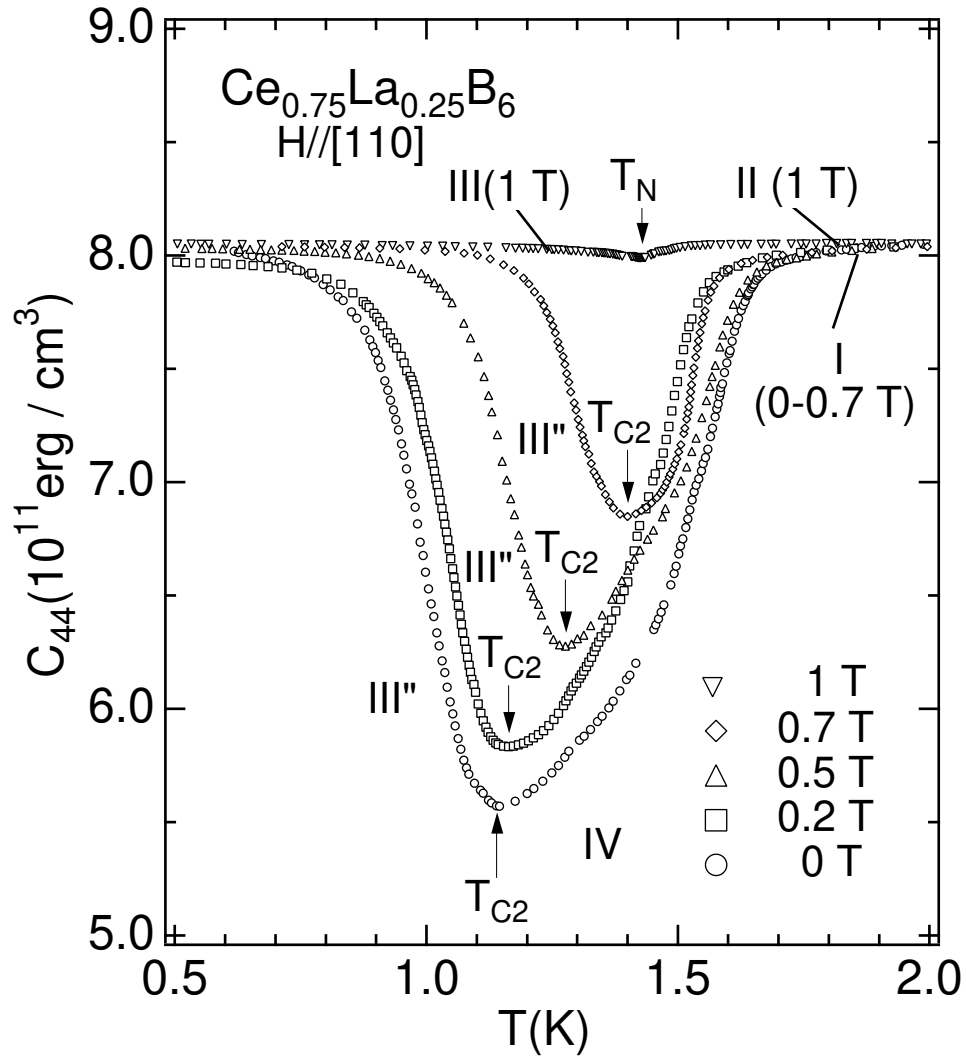


Fig. 2.

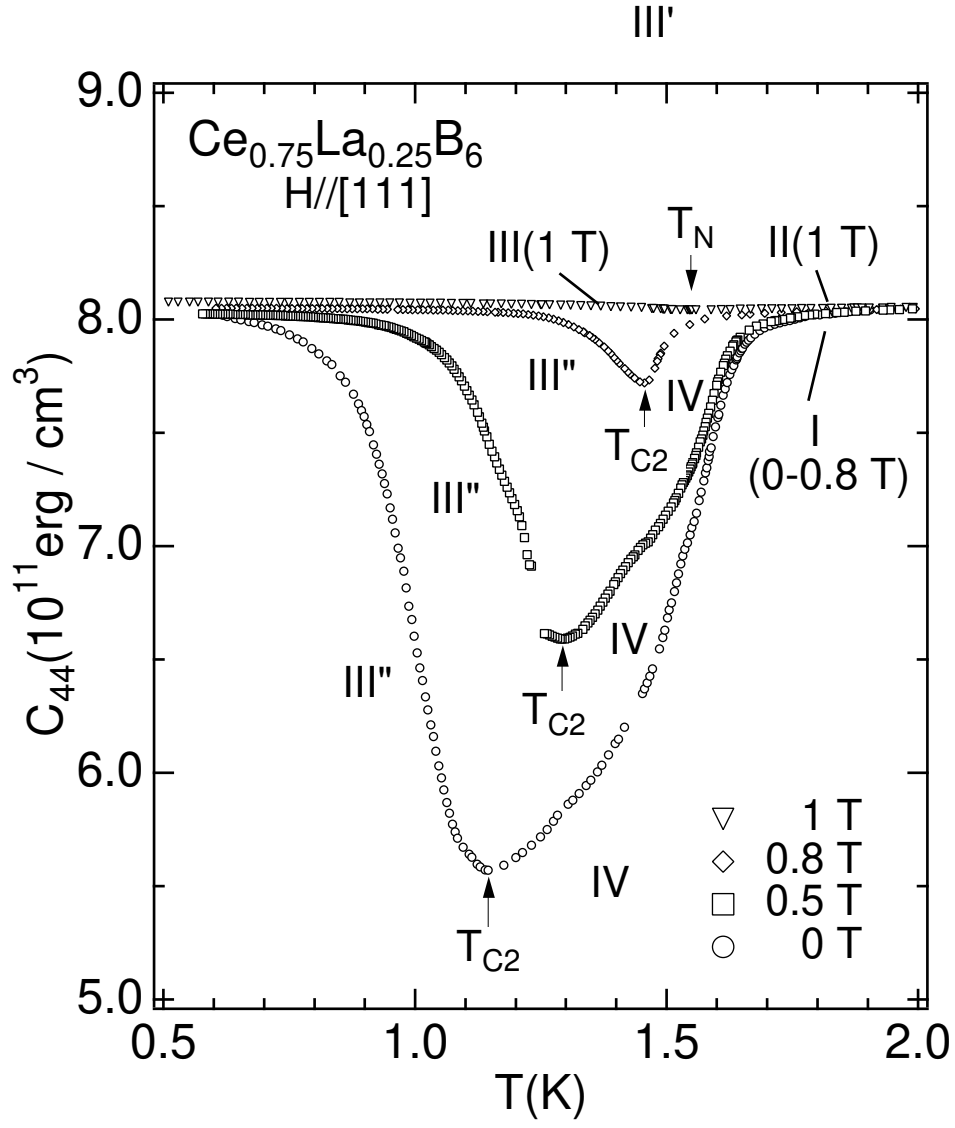


Fig. 3.

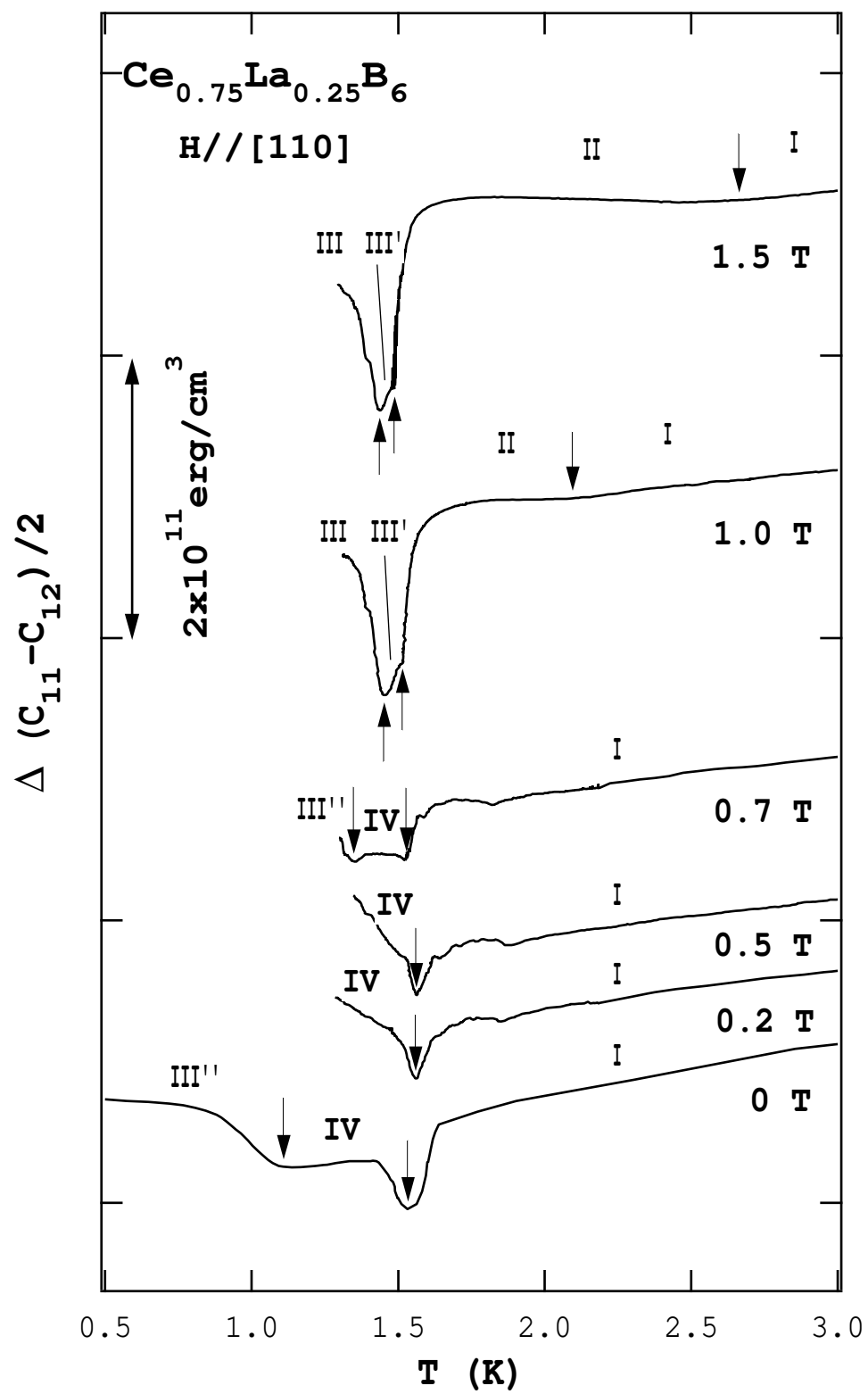


Fig. 4.

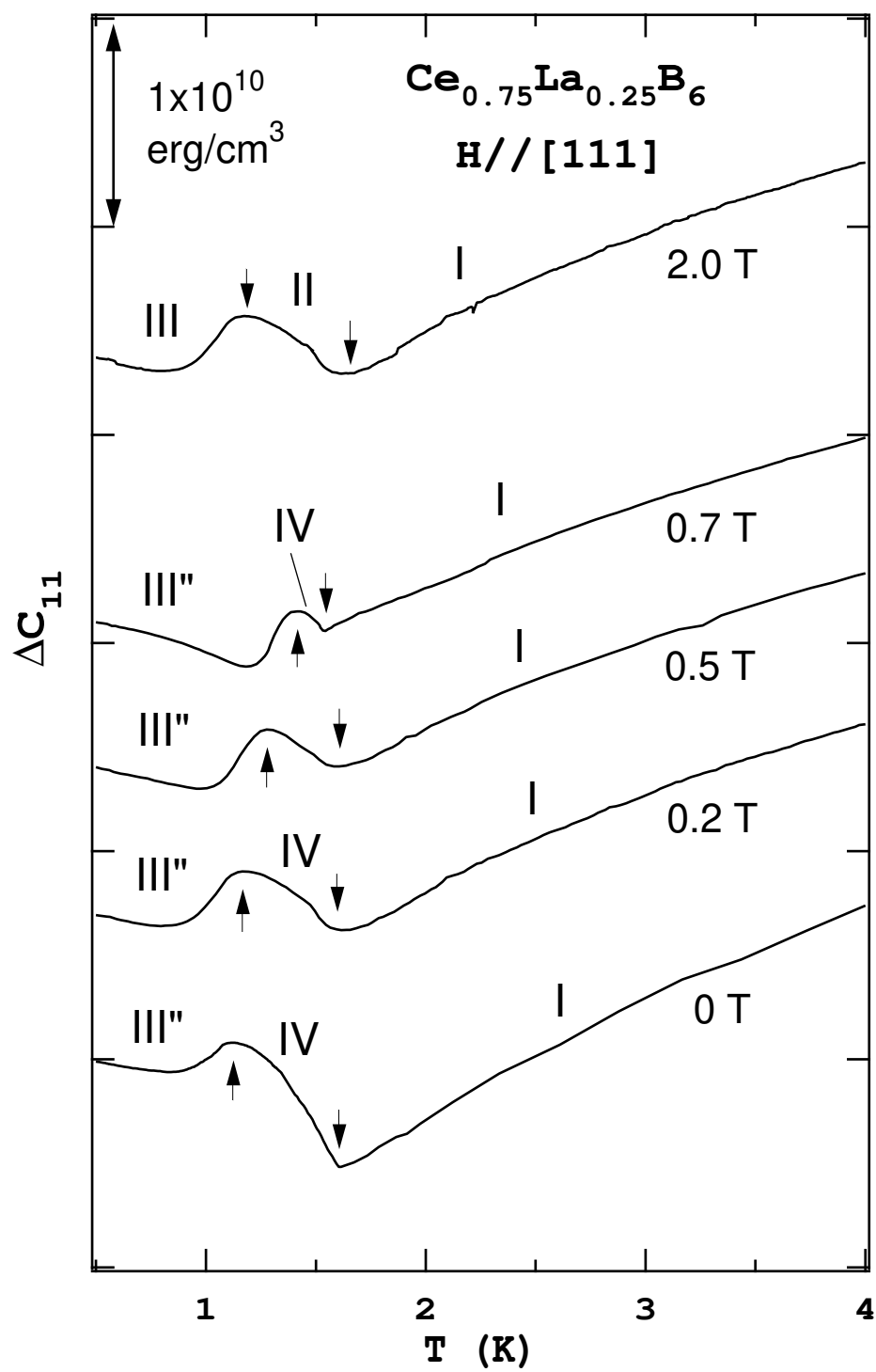


Fig. 5.

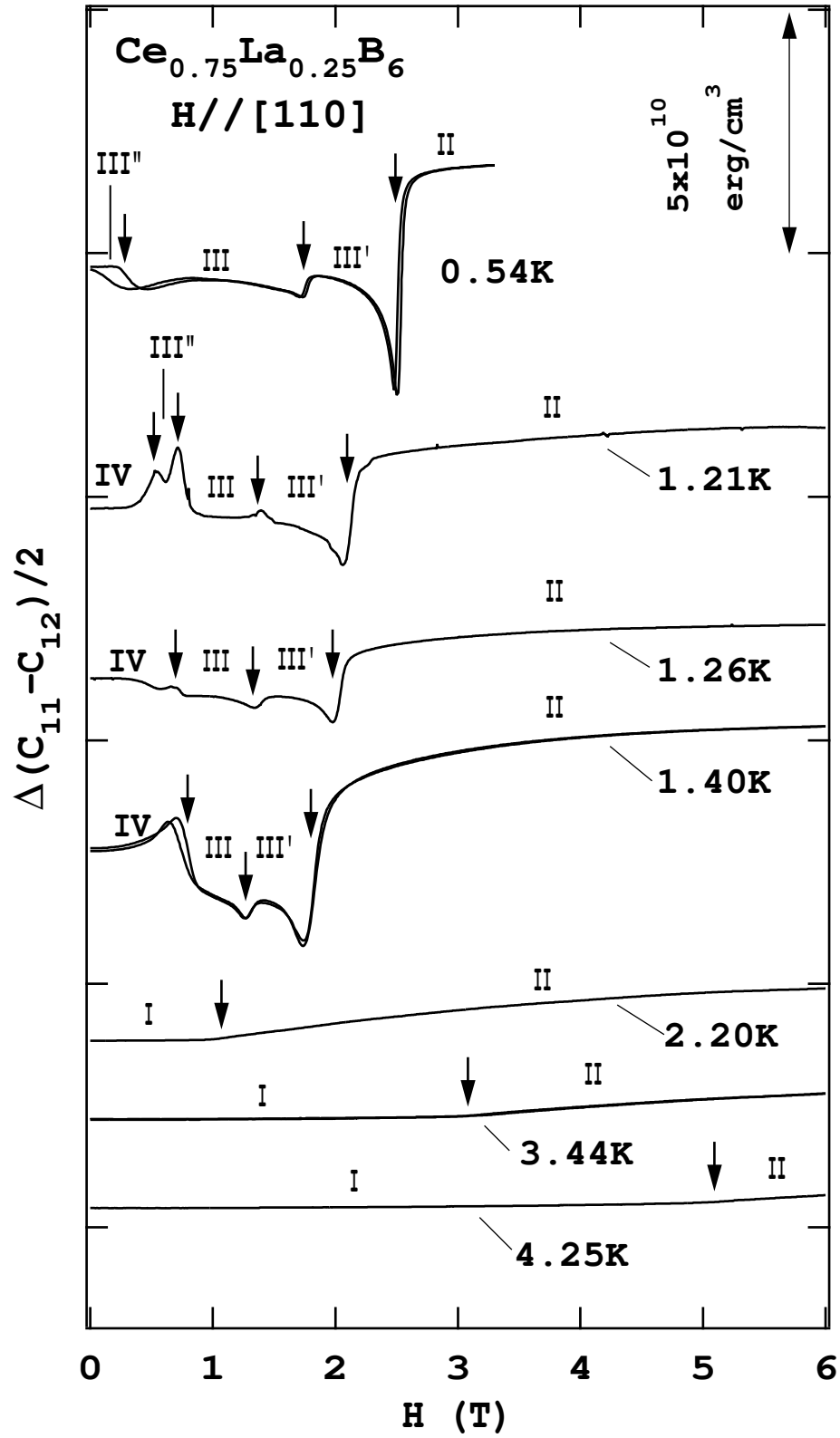


Fig. 6.

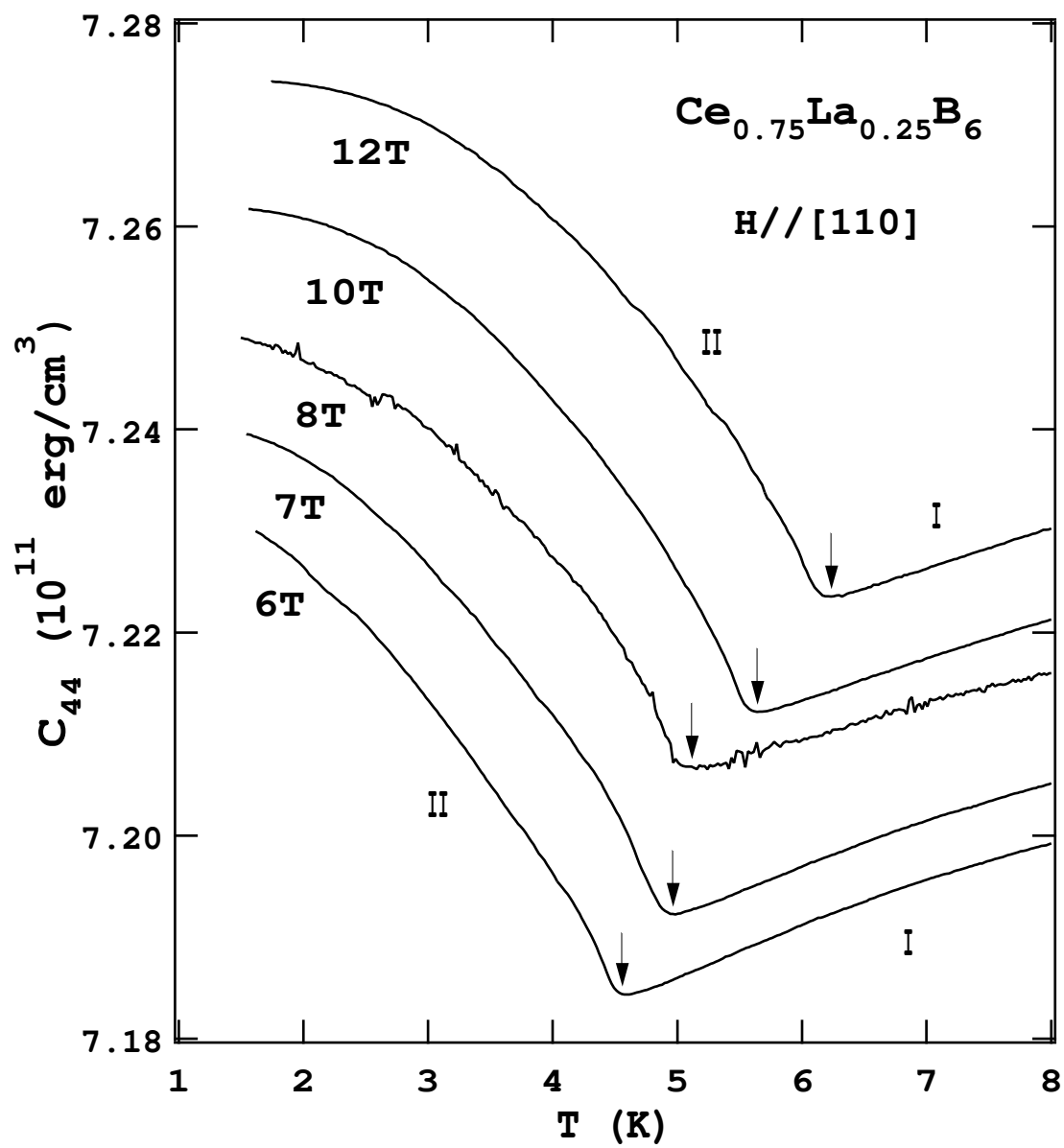


Fig. 7.

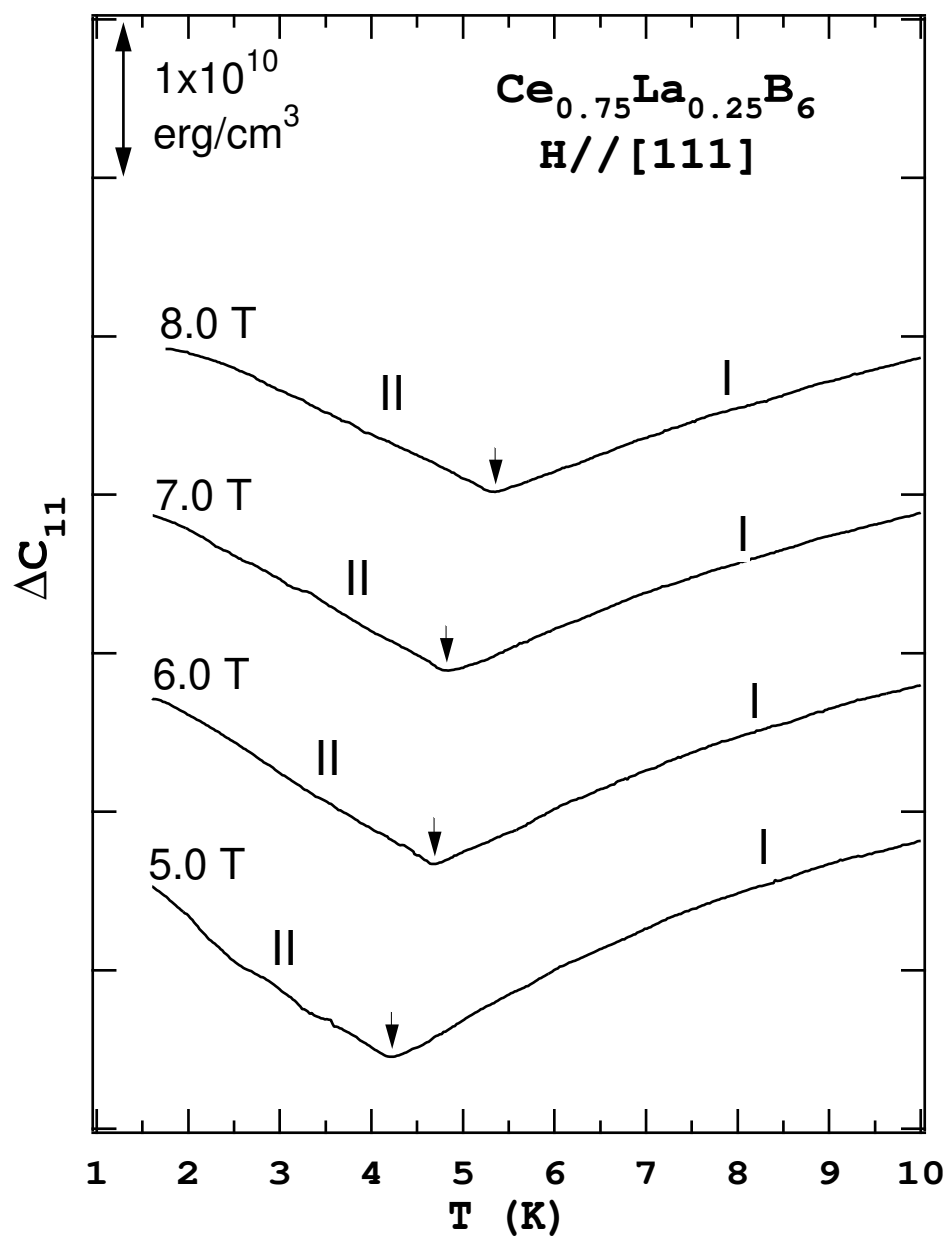


Fig. 8.

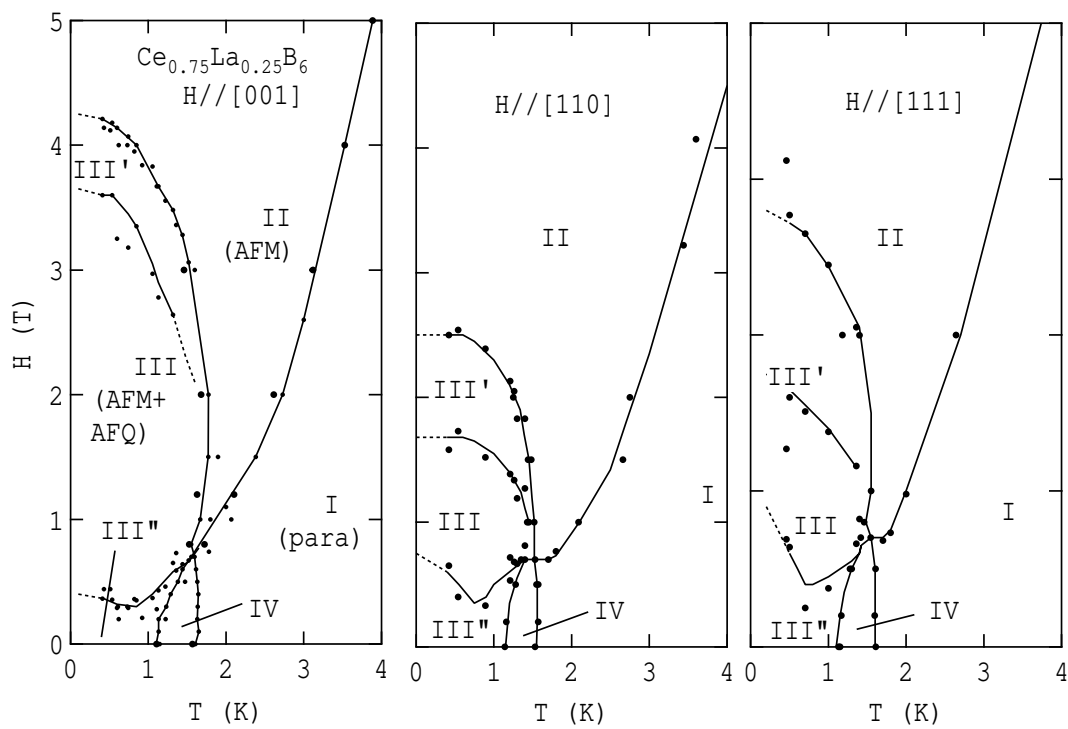


Fig. 9.